

Influence of current-voltage characteristic processing methods on the value of effective parameters of field cathodes

© A.G. Kolosko, S.V. Filippov, E.O. Popov

Ioffe Institute,
St. Petersburg, Russia
E-mail: agkolosko@mail.ru

Received May 12, 2023

Revised October 4, 2023

Accepted October 30, 2023

The paper analyzes the experimental current-voltage characteristics registered for a multitype nanocomposite field cathode based on carbon nanotubes. The analysis makes it possible to calculate effective estimates of the key parameters of field emission: the field enhancement factor and the emission area. A comparison of various approaches to analysis is presented, which include: various types of selection of a linear section on the current-voltage characteristic for constructing a trend line, various methods of averaging characteristics to eliminate the influence of the noise fluctuations, and the use of various coordinates for curve approximation.

Keywords: field emission, Fowler-Nordheim coordinates, trend line, effective parameters.

DOI: 10.61011/PSS.2023.12.57668.5126k

Comparison of the characteristics of dissimilar field cathodes is a key element in the process of optimizing their manufacturing technology. Characterization usually means recording current-voltage curves (IVC) and obtaining from them, using a trend line of effective parameters (EP): field enhancement factor (γ) and emission area (A). EP determination is complicated by a number of effects. The first effect is instability of emission properties. Even if the overall current level is stable, noise is observed in the recorded signal. This noise is associated with the measuring system and adsorption processes on the cathode surface in the vacuum chamber. The same noise leads to instability of IVC shape in time and to its unevenness [1,2]. The second effect is EP dependence on the choice of IVC section. This is especially typical for IVC, the shape of which significantly deviates from the chosen field emission law. This deviation can be associated both with adsorbates [1,2] and with the fact that the cathode consists of many emission sites of different shapes and relative positions [3]. Occasionally curvature of IVC and its noise tail is so strong that drawing a trend line leads to a huge error in the analysis [4,5]. In this case, it is necessary to select a straight section of IVC [6]. The third effect is the dependence of the result of the analysis of the experimental IVC on the selected coordinates: the primary coordinates I vs U (IU), Fowler-Nordheim coordinates $\ln(I/U^2)$ vs $1/U$ (FN), Millikan-Lauritsen coordinates $\ln I$ vs $1/U$ (ML) [7,8], as well as Murphy-Good coordinates [9] are used.

Note that in the case of multi-tip field cathodes, in addition to the difficulties of experimental determination of EP, the difficulty of their theoretical determination is also added. It is known that plotting the trend line in classical semi-logarithmic coordinates, even for ideal IVC of a single-tip model emitter, for example, in the form of a „hemisphere on a cylinder“ does not allow one to

restore with high accuracy the theoretical parameters such as the field enhancement factor at the apex (γ_0) and notional emission area ($A_0 = I/J_0$, where J_0 — current density at the apex). This error increases significantly when analyzing a cathode consisting of many such emitters. Moreover, to find the theoretical EPs of actual multi-tip cathode, it is necessary to know the exact geometry of its surface, which is practically impossible in the case of nanocomposite emitters.

The objective of this paper is to resolve the issue of choosing a method for EP assessing of a multi-tip field cathode. The methods were compared using the example of a study of actual cathode based on carbon nanoparticles. The criteria were the proximity of the resulting estimates to each other, as well as the magnitude of the error of their measurement. The novelty of the paper can be considered the presentation and comparison of various methods for IVC analysis, each of which is accessible and applicable in practice.

The experimental setup is a complex test unit with multi-channel recording of characteristics [10]. A specially developed program allows to plot IVC in real time, as well as to record them to a file and display them in emulation mode [11]. IVCs were measured in so-called „fast mode“: sample scanning with half-sinusoidal voltage pulses 20 ms wide, voltage amplitude $U_m = 1840 \pm 2.5$ V. One IVC consisting of 1000 points was recorded per one pulse. The area for analysis was selected from the point with number N_1 to the point with number N_2 . We fixed the number of the first point so that it was located next to the peak of the emission current ($N_1 = 430$). The number of the second point was selected using one of the methods that will be discussed below.

The sample was a nanocomposite of „multi-walled carbon nanotubes in a polystyrene polymer matrix“ (CNT/PS),

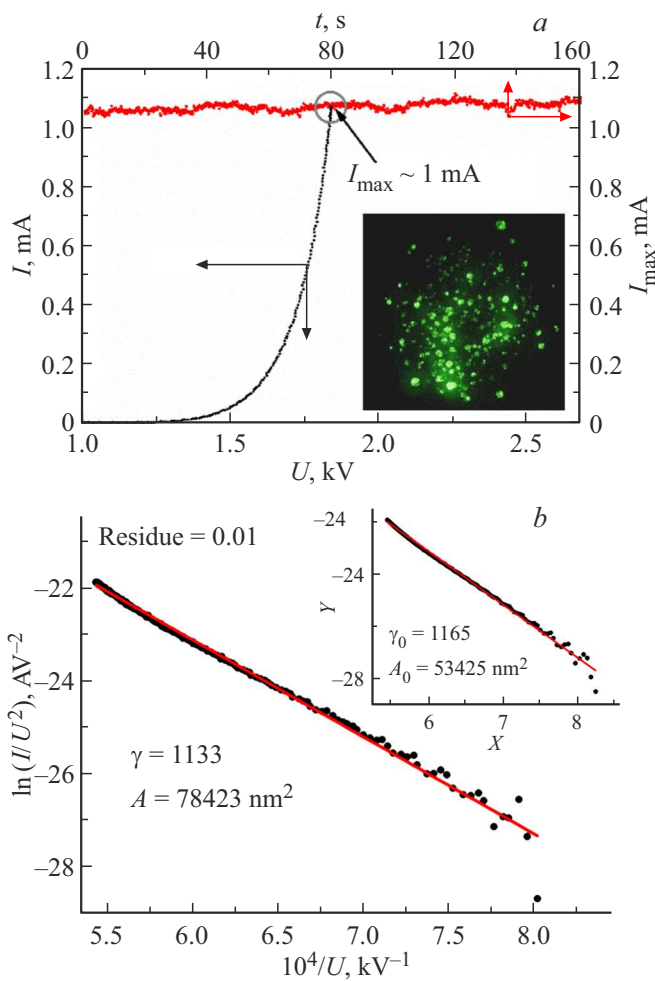


Figure 1. Experimental data for the CNT/PS field cathode, classical analysis: *a*) instantaneous IVC (decreasing voltage) and current level vs. time (the circle indicates the time moment when IVC was recorded), in the insert — profiles of voltage and current pulses; *b*) IVC in FN coordinates (selection of IVC section according to the principle of given deviation Residue = 0.01, analysis of the trend line in ES coordinates), in the insert — the same analysis for the time-averaged IVC.

deposited on a metal substrate with a diameter of 1 cm. The cathode was located at a distance $d = 370 \mu\text{m}$ from a flat metal anode of the same diameter in vacuum ($\approx 1 \cdot 10^{-7}$ Torr). The manufacturing process is described in paper [20]. According to the passport, CNT (Tuball brand, manufactured by Ltd OcSiAl, Novosibirsk) are single-walled $\sim 10 \mu\text{m}$ long.

Figure 1, *a* shows the measured characteristics of the cathode: the time dependence of the amplitude of the current pulses (the top point of IVC — I_{max}), the experimental IVC in the center of the time range in the coordinates IU and FN. Also a picture of the distribution of emission sites obtained using field projector with a fluorescent screen is presented.

Figure 1, *b* shows the result of the analysis using the classical ES approximation with plotting the trend line using the least squares method. The section selection corresponds

to Residue = 0.01 (mean-square deviation of IVC from the trend line).

The Elinson–Shrednik (ES) approximation gives the formula for the emission current [9]:

$$I = A \cdot (a_{FN}/1.1)\varphi^{-1} \exp(1.03b_{FN}c_S^2\varphi^{-1/2})d^{-2} \times U^2 \exp(-0.95b_{FN}\varphi^{3/2}d/(\gamma U)), \quad (1)$$

where A — emission area [m^2], a_{FN} and b_{FN} — first and second Fowler–Nordheim constants, c_S^2 — Schottky constant, $\varphi = 4.6 \text{ eV}$ — emitter work function.

Plotting trend line of type $y = a + bx$ in FN coordinates ($Y = \ln I/U^2$, $X = 1/U$) allows you to find EP cathode by slope b_{fit} and intercept a_{fit} :

$$\gamma = -d \cdot B_\varphi / b_{fit}, \quad (2)$$

$$A = \exp[a_{fit}](b_{fit})^2 / (A_\varphi B_\varphi^2), \quad (3)$$

where following is introduced

$$A_\varphi = 1.4\varphi^{-1} \exp(10.17\varphi^{-1/2}) \text{ and } B_\varphi = 6.49 \cdot 10^9 \varphi^{3/2}.$$

As a result of applying formulas (2) and (3) to IVC in Figure 1, the following EP values were obtained: $\gamma = 1133$ and $A = 78423 \text{ nm}^2$. We will take these parameters as basic ones for comparison with other options for analyzing experimental IVCs.

The recorded IVCs have a noise component. Let's consider averaging methods aimed at reducing the noise effect on the EP assessment. The first option is IVC averaging over time (MEAN-IVC). The control program has a built-in module that accumulates and averages the current and voltage values obtained for each of the 1000 pulse digitization points. The result of IVC analysis in the averaging mode is presented in the insert of Figure 1, *b*. Note that IVC averaging makes it smoother, which makes it possible to select a longer fragment of IVC for analysis. The second option for averaging is the accumulation and statistical analysis of EP (MEAN-EFF). Figure 2 shows the time dependences γ and A and their scattering diagrams. The values of the field enhancement factor γ determined using these two methods turned out to be quite close to each other (for MEAN-IVC $\gamma_0 = 1165$ and for MEAN-EFF $\gamma_{\text{mean}} = 1169$, $\sigma_{\gamma-\text{mean}} = 40$).

The emission area is calculated by placing the intercept value of the trend line into an exponential power, so it has increased sensitivity to noise and other deviations in IVC shape from the ideal exponent of the ES approximation. For both averaging methods it differs more than the enhancement factor (for MEAN-IVC $A_0 = 53425 \text{ nm}^2$, and for MEAN-EFF $A_{\text{mean}} = 57432 \text{ nm}^2$), however, the mean square deviation of its fluctuations is quite large $\sigma_{A-\text{mean}} = 24633 \text{ nm}^2$. Numerous studies show that such a large scattering in the estimate of the effective area when processing experimental data is generally characteristic of field cathodes (for example, [12]).

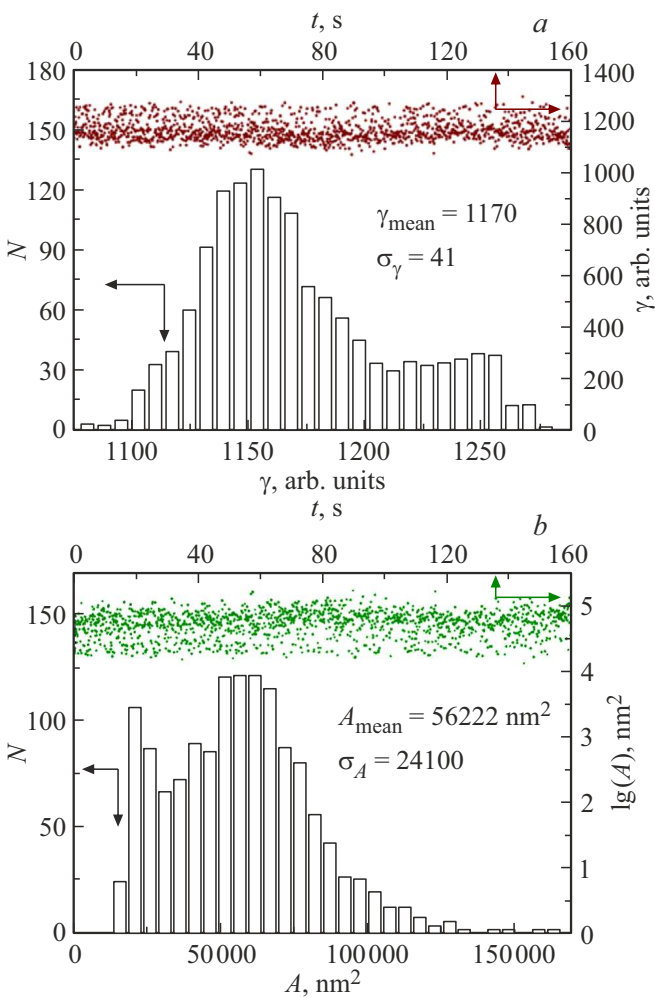


Figure 2. Stochastic fluctuations of effective parameters found along the trend line to IVC-PN, with selection of the analysis section using the method Residue = 0.01.

Let us consider methods for selecting IVC section for analysis. The first method — fixed deviation method (FixRes): IVC noise tail cut-off so that the root mean deviation from the Residue trend line is equal to a given value (Figure 1, b). The second method — fixed voltage method (FixUmin): the noise tail limit to a given voltage level U_{\min} . The third method — fixed length method (FixNum): fixing the number of points ΔN in the decreasing branch of IVC, i.e. start time t_1 and end time t_2 . The criteria for selecting the lower point of IVC section were chosen so that for all three methods these points were close to each other and located near the noise level boundary of the emission current signal: Residue = 0.01, $U_{\min} = 1200$ V and $N_2 = 580$.

Figure 3, a shows the profiles of current and voltage pulses and marks the points limiting IVC noise tail by the three methods described above (for clarity, the values of Residue, U_{\min} and ΔN in the Figure are selected so that the cursors are distinguishable).

Statistical analysis (using the MEAN-EFF method) made it possible to obtain EP for these three methods. These results are given in Table.

In all methods γ was found with an accuracy of $\sim 5\%$, but FixNum gave the minimum scattering. The value A has a much larger error than γ , about 50%, but even for it the most accurate method turned out to be FixNum.

Let's consider the use of different types of coordinates to construct plot trend line. We analyzed the instantaneous IVC in FN coordinates above (see Figure 1, b). Another option is to use ML coordinates ($\ln I$ vs $1/U$). The approximation of IVC in this case is carried out by the dependence $y = a - 2 \ln(x) + b \cdot x$, which corresponds to ES approximation (see (2)), and the calculation γ and A using the found a and b are made using the same formulas (2) and (3). The third option is to use of primary coordinates IU. The approximation of such a graph has the exponential form $y = x^2 \exp(a + b/x)$ and the same calculation γ and A using formulas (2) and (3).

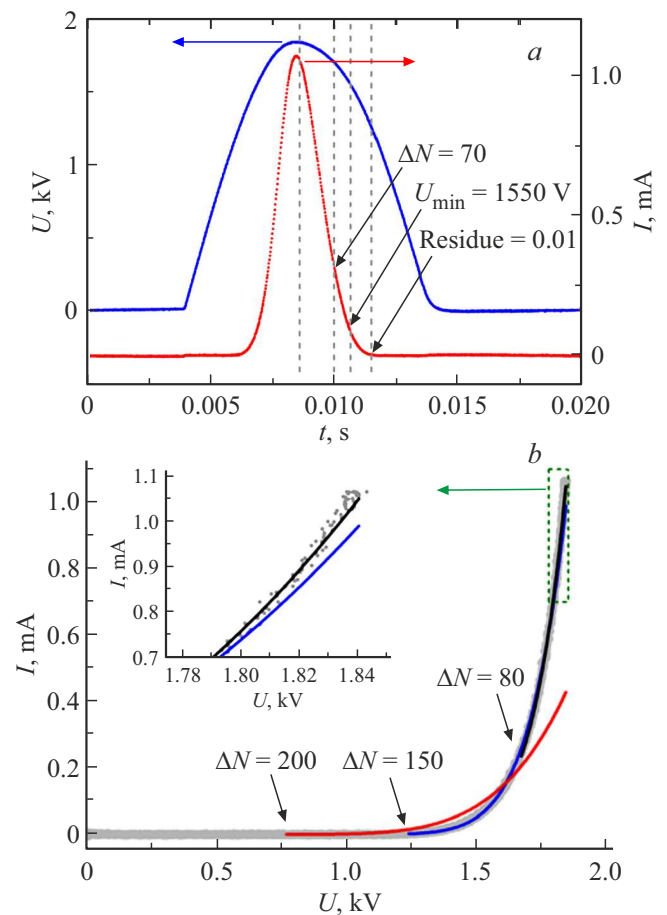


Figure 3. Selecting section and approximating IVC: a) profiles of current and voltage pulses indicating the points limiting the noise tail of IVC for arbitrary values of the parameters Residue, U_{\min} and ΔN , b) IVC approximation in IU coordinates for the selected segment $\Delta N = N_2 - N_1 = 80, 150, 200$ (the ends of the ranges — points N_2 are indicated by arrows). The insert shows enlarged apex of IVC; b) histograms of fluctuations of effective parameters for $\Delta N = 80$ and 150.

Results of EP assessment using different methods

Method of analysis of IVC section	Selection of section	γ	σ_γ	A , nm ²	σ_A , nm ²
One IVC in FN coordinates	FixRes Residue = 0.01	1133	–	78423	–
IVC averaging MEAN-IVC in FN coordinates	FixRes Residue = 0.01	1165	–	53425	–
EP averaging MEAN-EFF in FN coordinates	FixRes Residue = 0.01	1169	40	57432	24633
EP averaging MEAN-EFF in FN coordinates	FixUmin $U_{\min} = 1200$ V	1172	49	59589	38951
EP averaging MEAN-EFF in FN coordinates	FixNum $N_2 = 580$	1175	34	51907	21448

For comparison, all three types of coordinates FN, ML and IU were used for instantaneous IVCs on the segment of the same length ($N_1 = 430$, $N_2 = 580$). The approximating IVCs coincided with great accuracy, giving almost identical EPs $\gamma = 1175.07$ and $A = 51907$ nm². Thus, the choice of coordinates does not affect the EP value.

A special feature of using the exponential trend line in IU coordinates is that it allows one to include in the analysis IVC points that are in the noise tail and, due to fluctuations, occasionally take current value less than zero. Approximation in other coordinates (FN or ML), due to the use of the logarithm, requires either removing such IVC from the analysis or removing such points from the group.

Usually, experimenters do not assume about the change in EP when choosing other sections of IVC (unless at some voltage the slope of IVC does not change sharply), and the lower point of the range N_2 is chosen as close as possible to zero values of the emission current.

The nonlinearity of the experimental IVC in the FN coordinates leads to the fact that increase (decrease) in the sampling range, i.e. a shift of the point N_2 towards lower (higher) voltages gives a strong change in the EP values: the coefficient γ increases (decreases), and the area A decreases (increases), at the same time, the approximation deviation from the upper part of IVC increases (decreases). For example, for IVC obtained by the MEAN-EFF method when setting $N_2 = 510, 580, 630$, the EP values in IU coordinates are: $\gamma = 1021, 1175, 1868$ and $A = 352510, 51907, 241$ nm². Figure 3, *b* shows the corresponding approximation curves, where their strong discrepancy is visible.

We demonstrated this effect using the example of calculating EP of a multi-tip silicon emitter [13]. The curvature of IVC can be explained by the presence of a two-component distribution of emission sites according to the field enhancement factor [14]. A two-component distribution requires the use of approximation consisting of two curves with two sets of EP, but to date this approach was not automated and is almost never used by experimenters.

Note that EPs obtained in this paper (see Table) are quite consistent with the theoretical concepts of field cathodes with CNTs. The enhancement factor $\gamma \sim 1000$ is quite expected for a single CNT. The emission area of one CNT A_1 can be obtained by dividing the effective emission area of the cathode ($A \sim 50000$ nm²) by the number of emission sites. This number can be approximately estimated from the field projector pattern, where ~ 500 emission sites are observed. Then $A_1 = 100$ nm². From the paper [15] it follows that the effective emission area obtained using the Elinson–Shrednik approximation in FN coordinates for the physical model of CNTs can by two times exceed the conventional area. On the other hand, it was also shown there that the notional area depends on the dimensionless field, and in our range of fields it is approximately half of the cross-sectional area of the CNT. Thus, the effective area of one CNT can be related to the radius of the CNT: $A_1 = \pi \cdot r^2$. Then the radius of the CNT is $r \sim 5.6$ nm. This exceeds the permissible radius of single-walled CNTs (1 nm), and may be due to both the error of the measurements and the presence of inclusions of multi-walled CNTs on the cathode surface.

So, using the example of experimental data processing of nanocomposite cathode, we showed and compared various methods for IVC analysis. Two different signal averaging methods, i.e. MEAN-EFF and MEAN-IVC, gave rather close estimates. Thus, these methods are interchangeable. Methods of IVC section selection for FixRes, FixUmin and FixNum analysis showed a close scattering of parameters, but FixNum with the time interval fixation seemed to be the most accurate. The three types of coordinates IU, FN and ML showed identical results, and although IU allows you to include noise component in the analysis, it is recommended to limit the sampling to a threshold voltage, below which noise prevails in the signal, and negative current values appear.

Conflict of interest

The authors declare that they have no conflict of interest.

References

- [1] F. Giubileo, A. Di Bartolomeo, A. Scarfato, L. Iemmo, F. Bobba, M. Passacantando, S. Santucci, A.M. Cucolo. *Carbon* **47**, 4, 1074 (2009).
- [2] V. Guglielmotti, E. Tamburri, S. Orlanducci, M.L. Terranova, M. Rossi, M. Notarianni, S.B. Fairchild, B. Maruyama, N. Behabtu, C.C. Young, M. Pasquali. *Carbon* **52**, 356 (2013).
- [3] H.S. Jang, H.R. Lee, D.H. Kim. *Thin Solid Films* **500**, 1–2, 124 (2006).
- [4] L. Velasquez-Garcia. 43rd AIAA/ASME/SAE/ASEE Joint Propulsion Conference & Exhibit. USA, Cincinnati (08–11 July, 2007) OH, 5255-1.
- [5] K.L. Aplin, B.J. Kent, W. Song, C. Castelli. *Acta Astronautica* **64**, 9–10, 875 (2009).
- [6] S. Park, H.C. Kim, M.H. Yum, J.H. Yang, C.Y. Park, K. Chun, B. Eom, *Nanotechnology* **19**, 44, 445304-1 (2008).
- [7] M.M. Allaham, R.G. Forbes, A. Knápek, D. Sobola, D. Burda, P. Sedlak, M.S. Mousa. *Mater. Today Commun.* **31**, 103654-1 (2022).
- [8] D.P. Bernatski, V.G. Pavlov. *Tech. Phys.* **52**, 12, 1592(2007).
- [9] E.O. Popov, A.G. Kolosko, S.V. Filippov. *Tech. Phys. Lett.* **46**, 17, 838 (2020).
- [10] E.O. Popov, A.G. Kolosko, S.V. Filippov, E.I. Terukov, R.M. Ryazanov, E.P. Kitsyuk. *J. Vac. Sci. Technol. B* **38**, 4, 043203-1 (2020).
- [11] A.G. Kolosko, V.S. Chernova, S.V. Filippov, E.O. Popov. *Adv. Mater. Technol.* **3**, 18, 18 (2020).
- [12] A. Ayari, P. Vincent, S. Perisanu, P. Poncharal, S.T. Purcell. *J. Vac. Sci. Technol. B* **41**, 2, 024001-1 (2023).
- [13] A.G. Kolosko, S.V. Filippov, M.A. Chumak, E.O. Popov, G.D. Demin, I.D. Evsikov, N.A. Djuzhev. 19th Int. Conf. on Micro and Nanotechnology for Power Generation and Energy Conversion Applications. PowerMEMs 2019, Krakow, Poland, SubID: 82063205204 (2020).
- [14] E.O. Popov, A.G. Kolosko, S.V. Filippov, T.A. de Assis. *Vacuum* **173**, 109159-1 (2020).
- [15] S.V. Filippov, A.G. Kolosko, E.O. Popov. *IEEE Int. Vac. Electr. C* **64** (2023).

Translated by I.Mazurov